This article has been accepted for publication in IEEE Transactions on Intelligent Vehicles. This is the author's version which has not been fully edited and content may change prior to final publication. Citation information: DOI 10.1109/TIV.2022.3222009

Noncooperative Game-based Cooperative Maneuvering of Intelligent Surface Vehicles via Accelerated Learning-based Neural Predictors

Yibo Zhang, *Member, IEEE,* Wentao Wu, *Student Member, IEEE,* and Weidong Zhang, *Senior Member, IEEE*

***Abstract*—This paper investigates a noncooperative game-based cooperative maneuvering problem of multiple intelligent surface vehicles (ISVs) subject to uncertain nonlinearities and external disturbances. There exists a conflict between the overall objective of the swarm and own parameterized individual tasks of each ISV, resulting in a noncooperative game. A distributed cooperative maneuvering control method is proposed for multiple ISVs. Specifically, at first, action estimators are designed for each ISV based on the information of neighboring ISVs to estimate the actions of other ISVs. Then, an accelerated learning-based neural predictor is designed, where an echo state network is introduced as the identifier of uncertain nonlinearities, and adaptation laws are developed based on a high-order tuner to accelerate the convergence rate. Finally, controllers and update laws of individual variables are designed for multiple ISVs based on a distributed Nash equilibrium seeking approach, where the time derivative of the kinematic control law is obtained based on a nonlinear command filter. The control architecture is modular, leading to a decoupling of an action estimator module, a neural predictor module, and a controller module. Using the cascade system theory, the input-to-state stability of the resulting closed-loop system is guaranteed based on the input-to-state stability of three subsystems. A simulation example is provided to validate the effectiveness of the proposed noncooperative game-based distributed cooperative maneuvering control method.**

***Index Terms*—Intelligent surface vehicles, noncooperative game, cooperative maneuvering, Nash equilibrium seeking, accelerated learning-based neural predictor**

I. Introduction

INTELLIGENT surface vehicle (ISV), as an autonomous marine planform, is one of the intelligent vehicles family members [1]–[3]. Over the past two decades, advances on distributed cooperative control of multiple ISVs have provided efficient solutions for carrying out various maritime tasks, such as escorting, joint maritime rescuing, and water-quality sampling [4]–[7]. According to the guidance, the primary distributed cooperative control methods can be divided into time-related trajectories-guided tracking methods [8]–[11], moving targets-guided tracking methods [12]–[14], and parameterized paths-guided maneuvering methods [15]–[28].

Distributed cooperative maneuvering (also named cooperative path following in some literatures) of multiple ISVs guided by parameterized paths consists of two tasks [15], [16]. One is to develop controllers to drive these ISVs to achieve a coordinated motion guided by several parameterized paths and also known as a geometric task. Another one is to develop update laws for leader parameters to satisfy the desired assignments relating to time, velocity, or accelerate along these parameterized paths and also known as a dynamic task. In general, the geometric task has a higher priority than the dynamic task. In [17], [18], multiple parameterized paths-guided containment maneuvering problem is investigated for the ISVs swarm subject to unmodeled dynamics based on a state-feedback control scheme [17] and an output-feedback control scheme [18] separately. In [19], a path variable synchronization method is proposed for cooperative maneuvering of multiple surface vessels. In [20], a fuzzy adaptive controller is developed for distributed cooperative maneuvering of autonomous surface vehicles, where a command governor is designed by using a neural-dynamics optimization approach. On the basis of these methods in [17]–[20], many cooperative maneuvering control methods are proposed, such as event-triggered cooperative maneuvering [21], [22], data-driven adaptive cooperative maneuvering [22], [23], deep reenforcement learning-based cooperative maneuvering [24], vector field-based cooperative maneuvering [25], constraint cooperative maneuvering [26], and collision-free cooperative maneuvering [27], [28]. It should be noted that the above control methods [15]–[28] on distributed cooperative maneuvering of multiple ISVs focus on achieving the coordinated motion and formation configuration. During cooperative maneuvering, the desired motion or formation is the overall objective and can be implemented by developing appropriate control methods. However, in some practical applications, there may be not only the overall objective but also individual tasks for each ISV. The individual task of each ISV is usually independent of the overall objective. In general, the individual task may be private and cannot be accessed by other neighbors, resulting in the noncooperation of the swarm. In the marine search, multiple ISVs are guided by several parameterized paths to achieve a coordinated coverage. But due to the difference sub-tasks,

This paper is supported in part by Shanghai Science and Technology Program (22015810300, 19510745200), in part by Hainan Province Science and Technology Special Fund (ZDYF2021GXJS041), in part by the National Natural Science Foundation of China(U2141234, 52201369), and in part by the Hainan Special PhD Scientific Research Foundation of Sanya Yazhou Bay Science and Technology City under Grant HSPHDSRF-2022-01-007. (*Corresponding Author: Weidong Zhang*)

Yibo Zhang, Wentao Wu, and Weidong Zhang are with the Department of Automation, Shanghai Jiao Tong University, Shanghai 200240, China. Wentao Wu is also with SJTU Sanya Yazhou Bay Institute of Deepsea Science and Technology, Hainan, 572024, China. Weidong Zhang is also with the School of Information and Communication Engineering, Hainan University, Haikou 570228, Hainan, China. Email: {zhang297, wentao-wu, wdzhang}@sjtu.edu.cn.

This article has been accepted for publication in IEEE Transactions on Intelligent Vehicles. This is the author's version which has not been fully edited and content may change prior to final publication. Citation information: DOI 10.1109/TIV.2022.3222009

multiple ISVs may have the differences of moving position, velocity, and acceleration. These differences are private. It is challenging to develop distributed cooperative maneuvering controllers for the noncooperative ISVs swarm.

Noncooperative game theory is one of efficient tools to address the conflicts between the overall objective and the individual tasks [29]–[32]. In noncooperative games, all members in the swarm can be regarded as players. The payoff functions of each player are determined by the actions of the player as well as other players. During gaming, the payoff functions of each player are minimized based on its own actions, rather than the actions of all players. Recently, some Nash equilibrium seeking approaches are proposed for distributed equilibrium seeking by using the leader-following consensus protocol [29]–[31]. These works in [29]–[31] focus mainly on the numerical systems, and naturally extend to multiple ISVs [33], [34]. In [33], robust formation tracking of multiple ISVs with individual tasks is investigated, and the control objectives are transformed into a noncooperative game. In [34], a local noncooperative game-based placement problem is investigated for multiple ISVs under the quantized communication. These methods in [33], [34] are applicable to address the noncooperative game of multiple ISVs with respect to static or time-varying individual tasks. Noncooperative game-based cooperative maneuvering problem of multiple ISVs with parameterized individual tasks is still open.

Besides, there exist uncertain nonlinearities in the model of ISVs. In [15]–[20], adaptive identifiers are developed based on neural networks or fuzzy logic systems to approximate the uncertain nonlinearities. The adaptation laws in these methods [15]–[20] are developed by using a gradient descent method, where the convergence rate is influenced by many factors, such as initial conditions and persistency of excitation. Recently, an accelerated learning approach is developed based on the high-order tuner [35]–[37]. The accelerated learning-based adaptation has a higher convergence rate than the gradient-based adaptation, and thus the approximating speed of the adaptive identifier can be accelerated.

Motivated by the above observations mentioned, this paper is to develop a control method by using a distributed Nash equilibrium seeking approach for noncooperative game-based distributed cooperative maneuvering of multiple ASVs subject to uncertain nonlinearities and external disturbances. The proposed method is based on a modular design, consisting of consensus protocol-based action estimators, accelerated learning-based neural predictors, kinetic and kinematic control laws, and update laws of individual parameters. Compared with the existing control methods in [15]–[28], [33], [34], the main contributions of this paper can be concluded as follows

- In contrast to the cooperative maneuvering control methods in [15]–[28] proposed for multiple ISVs only with the overall objective, the cooperative maneuvering problem considered herein is with both the overall objective and individual tasks. A distributed cooperative maneuvering control method is proposed based on a distributed Nash equilibrium seeking approach to address the noncooperative game caused by the conflicts among different individual tasks.
- In contrast to the noncooperative game considered in [33], [34] with static or time-varying individual tasks, a noncooperative game-based cooperative maneuvering problem with parameterized individual tasks is investigated in this paper, where an individual parameter is introduced for each ISV as an additional degree of freedom. Especially, the noncooperative game considered herein can be regarded as a normal case of [33], [34].
- In contrast to the neural network-based or fuzzy logic system-based identifiers developed in [15]–[20] using a gradient descent adaptation, an accelerated learning-based neural predictor is constructed herein based on an echo state network and a high-order tuner approach, leading to a higher convergence rate.

The outline of this paper is as follows. Some preliminaries and the problem formulation are introduced in Section II. Section III presents the main design process of the control method for noncooperative game-based cooperative maneuvering. Section IV provides the main theoretical results. An application is introduced in Section V. The conclusions are formulated in Section VI.

II. Preliminaries and Problem Formulation

A. Notations

We use $\mathbb{R}^n$ and $\mathbb{R}^+$ to denote the n-dimensional Euclidean space and the positive real space respectively. $\|\cdot\|$ and $\|\cdot\|_{\mathrm{F}}$ are introduced to denote the Euclidean norm of a vector and the Frobenius norm of a matrix respectively. $\lambda_{\min}(\cdot)$ and $\lambda_{\max}(\cdot)$ are introduced to denote the minimum value and the maximum value of a matrix respectively. $\boldsymbol{I}_n$ represents an n-dimensional identity matrix. $\mathbf{0}_n$ represents an n-dimensional 0-vector. $\otimes$ represents the Kronecker product.

B. Noncooperative game

The swarm of ISVs considered in this paper is composed of M ISVs. In the distributed noncooperative game, the above M ISVs can be regraded as M players. Players receive actions from their neighbors by the distributed communication, which the topology can be described by using an undirected graph $\mathcal{G} = (\mathcal{N}, \mathcal{V}, \mathcal{E}, \boldsymbol{\mathcal{A}})$. $\mathcal{N} = \{1, ..., M\}$ stands for the set of players. $\mathcal{V} = (n_1, ..., n_M)$ stands for a vertex set with n_i denoting the ith node. $\varepsilon = \{(n_i, n_j) \in \mathcal{V} \times \mathcal{V}\}$ stands for an edge set with $(n_i, n_j) \in \varepsilon$ being an action access from the jth player to the ith player. $\boldsymbol{\mathcal{A}} = [a_{i,j}] \in \mathbb{R}^{M\times M}$ denotes an adjacency matrix, where $a_{i,j} = 1$ means $(n_i, n_j) \in \mathcal{E}$ and $a_{i,j} = 0$ means $(n_i, n_j) \notin \mathcal{E}$. Furthermore, a Laplacian matrix of $\mathcal{G}$ is defined as $\boldsymbol{\mathcal{L}} \in \mathbb{R}^{M\times M} := \boldsymbol{D} - \boldsymbol{\mathcal{A}}$, where $\boldsymbol{D} = \mathrm{diag}\{d_1, ..., d_M\}$ with $d_i = \sum_{j\in\mathcal{N}_i} a_{i,j}$ denotes a degree matrix and $\mathcal{N}_i = \{j | (n_i, n_j) \in \mathcal{E}\}$ denotes a neighbor set of the ith player.

For a game objective of the ith player, a payoff function is defined as $J_i(\boldsymbol{u}) : \mathbb{R}^{Mm} \to \mathbb{R}$ with $\boldsymbol{u} = [\boldsymbol{u}_1^{\mathrm{T}}, ..., \boldsymbol{u}_M^{\mathrm{T}}]^{\mathrm{T}}$ and m being the dimension of the action $\boldsymbol{u}_i$. The payoff function $J_i(\boldsymbol{u})$ could be minimized by adjusting the action $\boldsymbol{u}_i$. It is assumed that the payoff functions of all players could be minimized spontaneously, such that

$$J_i(\boldsymbol{u}_i, \boldsymbol{u}_{-i}^*) \geq J_i(\boldsymbol{u}_i^*, \boldsymbol{u}_{-i}^*),$$

This article has been accepted for publication in IEEE Transactions on Intelligent Vehicles. This is the author's version which has not been fully edited and content may change prior to final publication. Citation information: DOI 10.1109/TIV.2022.3222009

where $\boldsymbol{u}_i^* \in \mathbb{R}^m$ is a solution of the distributed noncooperative game and also called as a Nash equilibrium solution, and $\boldsymbol{u}_{-i}^* = [\boldsymbol{u}_1^{*\mathrm{T}}, ..., \boldsymbol{u}_{i-1}^{*\mathrm{T}}, \boldsymbol{u}_{i+1}^{*\mathrm{T}}, ..., \boldsymbol{u}_M^{*\mathrm{T}}]^{\mathrm{T}} \in \mathbb{R}^{(M-1)m}$. It is noted that there exists at least one Nash equilibrium solution in the distributed noncooperative game if $J_i(\boldsymbol{u})$ is convex and continuous differentiable. Nash equilibrium $\boldsymbol{u}_i^* \in \mathbb{R}^m$ satisfies $\partial J_i(\boldsymbol{u})/\boldsymbol{u}_i^* = \boldsymbol{0}_m$.

Definition 1. **[38]** An action profile, as a Nash equilibrium, means that no player can reduce its payoff by unilaterally changing its own action. That is, an action profile $\boldsymbol{u}^* = [\boldsymbol{u}_1^{*\mathrm{T}}, ..., \boldsymbol{u}_M^{*\mathrm{T}}]^{\mathrm{T}}$ is the Nash equilibrium if all players satisfies $J_i(\boldsymbol{u}_i, \boldsymbol{u}_{-i}^*) \geq J_i(\boldsymbol{u}_i^*, \boldsymbol{u}_{-i}^*)$.

C. Problem formulation

Consider the following kinematics of the ith ISV as

$$\begin{cases} \dot{\boldsymbol{\eta}}_i = \boldsymbol{R}(\psi_i)\boldsymbol{\nu}_i, \ i = 1, ..., M \\ \boldsymbol{R}_i = \begin{bmatrix} \cos(\psi_i) & -\sin(\psi_i) & 0 \\ \sin(\psi_i) & \cos(\psi_i) & 0 \\ 0 & 0 & 1 \end{bmatrix} \end{cases} \tag{1}$$

and the following kinetics of the ith ISV as

$$\boldsymbol{M}_i\dot{\boldsymbol{\nu}}_i = \boldsymbol{\tau}_i + \boldsymbol{f}_i(\boldsymbol{\nu}_i) + \boldsymbol{w}_i(t) \tag{2}$$

where $\boldsymbol{\eta}_i = [x_i, y_i, \psi_i]^{\mathrm{T}} \in \mathbb{R}^3$ is a vector consisting of positions and the heading angle in the earth-fixed coordinate system, $\boldsymbol{\nu}_i = [u_i, v_i, r_i]^{\mathrm{T}} \in \mathbb{R}^3$ denotes a vector consisting of the surge, sway, and yaw velocities in the body-fixed coordinate system, $\boldsymbol{M}_i \in \mathbb{R}^{3\times3}$ is a diagonal inertia matrix, $\boldsymbol{f}_i(\boldsymbol{\nu}_i) \in \mathbb{R}^3$ denotes an unknown nonlinear terms affected by Coriolis and centripetal forces, hydrodynamics, unknown damping, and unmodeled dynamics, $\boldsymbol{\tau}_i \in \mathbb{R}^3$ represents a vector consisting of control torques and moment, and $\boldsymbol{w}_i(t) \in \mathbb{R}^3$ is a bounded environmental disturbance. Two different coordinate systems are shown in Fig. 1.

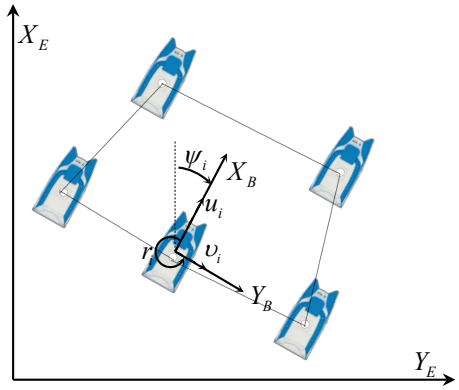

Fig. 1: Two coordinate systems ($X_E - Y_E$: Earth-fixed coordinate system; $X_B - Y_B$: Body-fixed coordinate system)

If there exists the Nash equilibrium in the distributed noncooperative game, a Nash equilibrium seeking strategy can be developed. Different from the existing works in [33], [34], the distributed noncooperative game considered herein is constructed based on cooperative maneuvering, where the payoff function herein is designed by using additional parameterized individual objectives. This paper is to develop a Nash equilibrium seeking strategy-based cooperative maneuvering controller for each player to achieve the following two tasks

- *Geometric Task:* The output $\boldsymbol{\eta}_i$ is regarded as an action of the ith player. Each player is driven to minimize a quadratic payoff function as follows

$$\min \sum_{i=1}^{M} J_{i,1}(\boldsymbol{\eta}, \boldsymbol{\eta}_{\mathrm{r},i}(\theta_i)) \tag{3}$$

  where $\boldsymbol{\eta} = [\boldsymbol{\eta}_1^{\mathrm{T}}, ..., \boldsymbol{\eta}_M^{\mathrm{T}}]^{\mathrm{T}} \in \mathbb{R}^{3M}$, $\boldsymbol{\eta}_{\mathrm{r},i}(\theta_i) \in \mathbb{R}^3$ denotes a parameterized individual objective, and $\theta_i \in \mathbb{R}$ denotes an individual parameter of the ith player satisfying $\dot{\theta}_i = \tau_{\mathrm{p},i}$ with $\tau_{\mathrm{p},i}$ is a to-be-designed parameter update law. Letting $g_{i,1}(\boldsymbol{\eta}) = \partial J_{i,1}(\boldsymbol{\eta}, \boldsymbol{\eta}_{\mathrm{r},i}(\theta_i))/\partial\boldsymbol{\eta}_i$, any Nash Equilibriums $\boldsymbol{\eta}^*$ satisfy

$$g_{i,1}(\boldsymbol{\eta}^*) = \boldsymbol{0}_3 \tag{4}$$

  where $\boldsymbol{\eta}^* = [\boldsymbol{\eta}_1^{*\mathrm{T}}, ..., \boldsymbol{\eta}_M^{*\mathrm{T}}]^{\mathrm{T}} \in \mathbb{R}^{3M}$.
- *Dynamic Task:* The individual parameter θ_i is regarded as an action of the ith player. Each player is driven to minimize a quadratic payoff function as follows

$$\min \sum_{i=1}^{M} J_{i,2}(\boldsymbol{\theta}) \tag{5}$$

  where $\boldsymbol{\theta} = [\theta_1, ..., \theta_M]^{\mathrm{T}} \in \mathbb{R}^M$.
  Letting $g_{i,2}(\boldsymbol{\theta}) = \partial J_{i,2}(\boldsymbol{\theta})/\partial\theta_i$, any Nash equilibriums $\boldsymbol{\theta}^*$ satisfy

$$g_{i,2}(\boldsymbol{\theta}^*) = 0 \tag{6}$$

  where $\boldsymbol{\theta}^* = [\theta_1^*, ..., \theta_M^*]^{\mathrm{T}} \in \mathbb{R}^M$.

Assumption 1. The communication topology among players is undirected and connected.

Assumption 2. **[29]** For all $i \in \mathcal{N}$, there exists at least one Nash equilibrium $\boldsymbol{\eta}^*$ and $\boldsymbol{\theta}^*$ satisfying the following two conditions

$$\frac{\partial J_{i,1}(\boldsymbol{\eta}^*, \boldsymbol{\eta}_{\mathrm{r},i}(\theta_i))}{\partial\boldsymbol{\eta}_i} = 0, \ \frac{\partial^2 J_{i,1}(\boldsymbol{\eta}^*, \boldsymbol{\eta}_{\mathrm{r},i}(\theta_i))}{\partial\boldsymbol{\eta}_i^2} < 0 \tag{7}$$

and

$$\frac{\partial J_{i,2}(\boldsymbol{\theta}^*)}{\partial\theta_i} = 0, \ \frac{\partial^2 J_{i,2}(\boldsymbol{\theta}^*)}{\partial\theta_i^2} < 0. \tag{8}$$

Assumption 3. **[32], [39], [40]** There exists a constant $\varrho_l \in \mathbb{R}^+$ such that

$$\|g_i(\boldsymbol{a}) - g_i(\boldsymbol{b})\| \leq \varrho_l\|\boldsymbol{a} - \boldsymbol{b}\|$$

holds for any $\boldsymbol{a}, \boldsymbol{b} \in \mathbb{R}^m$.

Remark 1. When mixed actions are allowed, there exists at least one Nash equilibrium if each noncooperative game with a finite number of players in which each player can choose from finitely many actions. This property can be proved by Brouwer's fixed-point theorem and Kakutani's fixed-point theorem. Furthermore, Ref. [29] has proved that when *Assumption 2* is satisfied for the noncooperative game with quadratic payoff functions, the Nash equilibrium solution of the considered

noncooperative game is unique. Quadratic payoff functions can be used to describe many cooperative behaviors [29], [41], such as formation, flocking, and surrounding.

Remark 2. Recently, many cooperative maneuvering control methods [15]–[28] are proposed from different angles, such as leader properties, limited resources, intelligent methods, and collision avoidance. These methods [15]–[28] are developed to achieve the desired motion or formation, where is as the overall objective considered in the noncooperative game-based cooperative maneuvering. But, noncooperative individual tasks are not considered in these results.

III. Nash equilibrium seeking strategy-based cooperative maneuvering controller design

A. Action estimators based on the consensus protocol

In the distributed noncooperative game, the player is unable to obtain the actions of the non-neighboring players directly. Accordingly, distributed action estimators can be introduced to estimate the actions of other non-neighboring players by using the information from its neighboring players. The following distributed action estimator is developed to estimate the action $\boldsymbol{\eta}_j$ based on a consensus protocol in [29] as

$$\dot{\hat{\boldsymbol{\eta}}}_{i,j} = -\boldsymbol{\mu}_{i,j}[\sum_{k\in\mathcal{N}_i} a_{i,k}(\hat{\boldsymbol{\eta}}_{i,j} - \hat{\boldsymbol{\eta}}_{k,j}) + a_{i,j}(\hat{\boldsymbol{\eta}}_{i,j} - \boldsymbol{\eta}_j)] \quad (9)$$

where $\boldsymbol{\mu}_{i,j} \in \mathbb{R}^{3\times 3}$ denotes a positive definite tuning parameter matrix, $\hat{\boldsymbol{\eta}}_{i,j} \in \mathbb{R}^3$ denotes an estimated action of the ith player, $\hat{\boldsymbol{\eta}}_{k,j} \in \mathbb{R}^3$ denotes an estimated action of the kth player, $\mathcal{N}_i$ is the neighbor set of the ith player, and $a_{i,k}$ and $a_{i,j}$ are adjacency weights defined in *Section* II.

Similarly, a distributed action estimator is developed to estimate the action θ_j as follows

$$\dot{\hat{\theta}}_{i,j} = -\kappa_{i,j}[\sum_{k\in\mathcal{N}_i} a_{i,k}(\hat{\theta}_{i,j} - \hat{\theta}_{k,j}) + a_{i,j}(\hat{\theta}_{i,j} - \theta_j)] \quad (10)$$

where $\kappa_{i,j} \in \mathbb{R}^+$ denotes a tuning parameter, $\hat{\theta}_{i,j} \in \mathbb{R}$ denotes an estimated action of the ith player, $\hat{\theta}_{k,j} \in \mathbb{R}$ denotes an estimated action of the kth player.

Define $\hat{\boldsymbol{\eta}}_i = [\hat{\boldsymbol{\eta}}_{i,1}^{\mathrm{T}}, ..., \hat{\boldsymbol{\eta}}_{i,M}^{\mathrm{T}}]^{\mathrm{T}} \in \mathbb{R}^{3M}$ and $\boldsymbol{\eta} = [\boldsymbol{\eta}_1^{\mathrm{T}}, ..., \boldsymbol{\eta}_M^{\mathrm{T}}]^{\mathrm{T}} \in \mathbb{R}^{3M}$, and one yields that

$$\dot{\hat{\boldsymbol{\eta}}}_i = -\boldsymbol{\mu}_i[\sum_{k\in\mathcal{N}_i} a_{i,k}(\hat{\boldsymbol{\eta}}_i - \hat{\boldsymbol{\eta}}_k) + (\boldsymbol{\Lambda}_i \otimes \boldsymbol{I}_3)(\hat{\boldsymbol{\eta}}_i - \boldsymbol{\eta})] \quad (11)$$

where $\boldsymbol{\mu}_i = \mathrm{diag}\{\boldsymbol{\mu}_{i,1}, ..., \boldsymbol{\mu}_{i,M}\} \in \mathbb{R}^{3M\times 3M}$ and $\boldsymbol{\Lambda}_i = \mathrm{diag}\{a_{i,1}, ..., a_{i,M}\} \in \mathbb{R}^{M\times M}$.

Define $\hat{\boldsymbol{\theta}}_i = [\hat{\theta}_{i,1}, ..., \hat{\theta}_{i,M}]^{\mathrm{T}} \in \mathbb{R}^M$ and $\boldsymbol{\theta} = [\theta_1^{\mathrm{T}}, ..., \theta_M^{\mathrm{T}}]^{\mathrm{T}} \in \mathbb{R}^M$, and it follows that

$$\dot{\hat{\theta}}_i = -\boldsymbol{\kappa}_i[\sum_{k=1}^{M} a_{i,k}(\hat{\boldsymbol{\theta}}_i - \hat{\boldsymbol{\theta}}_k) + \boldsymbol{\Lambda}_i(\hat{\boldsymbol{\theta}}_i - \boldsymbol{\theta})] \quad (12)$$

where $\boldsymbol{\kappa}_i = \mathrm{diag}\{\kappa_{i,1}, ..., \kappa_{i,M}\} \in \mathbb{R}^{M\times M}$.

Define $\tilde{\boldsymbol{\eta}} = \hat{\boldsymbol{\eta}} - \mathbf{1}_M \otimes \boldsymbol{\eta}$ with $\hat{\boldsymbol{\eta}} = [\hat{\boldsymbol{\eta}}_1^{\mathrm{T}}, ..., \hat{\boldsymbol{\eta}}_M^{\mathrm{T}}]^{\mathrm{T}} \in \mathbb{R}^{3MM}$. The dynamics of $\tilde{\boldsymbol{\eta}}$ is given by

$$\dot{\tilde{\boldsymbol{\eta}}} = -\boldsymbol{\mu}(\boldsymbol{H} \otimes \boldsymbol{I}_3)\tilde{\boldsymbol{\eta}} - \mathbf{1}_M \otimes \dot{\boldsymbol{\eta}} \quad (13)$$

where $\boldsymbol{\mu} = \mathrm{diag}\{\boldsymbol{\mu}_1, ..., \boldsymbol{\mu}_M\} \in \mathbb{R}^{3MM\times 3MM}$ and $\boldsymbol{H} = \boldsymbol{\mathcal{L}} \otimes \boldsymbol{I}_M + \boldsymbol{\Lambda}$ with $\boldsymbol{\Lambda} = \mathrm{diag}\{\boldsymbol{\Lambda}_1, ..., \boldsymbol{\Lambda}_M\} \in \mathbb{R}^{MM\times MM}$.

Define $\tilde{\boldsymbol{\theta}} = \hat{\boldsymbol{\theta}} - \mathbf{1}_M \otimes \boldsymbol{\theta}$ with $\hat{\boldsymbol{\theta}} = [\hat{\boldsymbol{\theta}}_1^{\mathrm{T}}, ..., \hat{\boldsymbol{\theta}}_M^{\mathrm{T}}]^{\mathrm{T}} \in \mathbb{R}^{MM}$. The dynamics of $\tilde{\boldsymbol{\theta}}$ is given by

$$\dot{\tilde{\boldsymbol{\theta}}} = -\boldsymbol{\kappa}\boldsymbol{H}\tilde{\boldsymbol{\theta}} - \mathbf{1}_M \otimes \dot{\boldsymbol{\theta}} \quad (14)$$

where $\boldsymbol{\kappa} = \mathrm{diag}\{\boldsymbol{\kappa}_1, ..., \boldsymbol{\kappa}_M\} \in \mathbb{R}^{M\times M}$.

At last, the dynamics of the subsystem consisting of $\tilde{\boldsymbol{\eta}}$ and $\tilde{\boldsymbol{\theta}}$ is given by the following form

$$\begin{cases} \dot{\tilde{\boldsymbol{\eta}}} = -\boldsymbol{\mu}(\boldsymbol{H} \otimes \boldsymbol{I}_3)\tilde{\boldsymbol{\eta}} - \mathbf{1}_M \otimes \dot{\boldsymbol{\eta}} \\ \dot{\tilde{\boldsymbol{\theta}}} = -\boldsymbol{\kappa}\boldsymbol{H}\tilde{\boldsymbol{\theta}} - \mathbf{1}_M \otimes \dot{\boldsymbol{\theta}}. \end{cases} \quad (15)$$

B. Neural predictors based on accelerated learning

In this subsection, a neural predictor is proposed based on the accelerated learning approach. At first, recall the kinetics of the ith ISV as follows

$$\dot{\boldsymbol{\nu}}_i = \boldsymbol{F}_i(\boldsymbol{\nu}_i, t) + \boldsymbol{M}_i^{-1}\boldsymbol{\tau}_i \quad (16)$$

where $\boldsymbol{F}_i(\boldsymbol{\nu}_i, t) = \boldsymbol{f}_i(\boldsymbol{\nu}_i) + \boldsymbol{w}_i(t)$.

Because $\boldsymbol{F}_i(\cdot)$ is an uncertain nonlinear term, the following echo state network is introduced to approximate this term [42]

$$\boldsymbol{F}_i(\cdot) = \boldsymbol{W}_i^{*\mathrm{T}}\boldsymbol{X}_i + \boldsymbol{\varepsilon}_i \quad (17)$$

where $\boldsymbol{W}_i^* \in \mathbb{R}^{m\times 3}$ is the ideal output weights matrix of echo state network with m being the dimensional of the reservoir $\boldsymbol{X}_i \in \mathbb{R}^m$ and $\boldsymbol{\varepsilon}_i \in \mathbb{R}^3$ denotes an approximation error satisfying $\|\boldsymbol{\varepsilon}_i\| \leq \varepsilon_i^*$ with $\varepsilon_i^* \in \mathbb{R}^+$. The dynamics of $\boldsymbol{X}_i$ is given as follows

$$\dot{\boldsymbol{X}}_i = c_i(-b_i\boldsymbol{X}_i + \sigma(\boldsymbol{W}_{\boldsymbol{\xi},i}\boldsymbol{\xi}_i + \boldsymbol{W}_{\boldsymbol{X},i}\boldsymbol{X}_i))$$

where $c_i \in \mathbb{R}^+$ is a time constant, $b_i \in \mathbb{R}^+$ is a leaking decay rate, $\boldsymbol{\xi}_i = [\boldsymbol{\nu}_i^{\mathrm{T}}(t), \boldsymbol{\nu}_i^{\mathrm{T}}(t-t_{\mathrm{d}}), \boldsymbol{u}_i^{\mathrm{T}}(t)]^{\mathrm{T}} \in \mathbb{R}^9$ is the input vector of the echo state network with $t_{\mathrm{d}} \in \mathbb{R}^+$ being a sampling interval, $\sigma(\cdot) : \mathbb{R}^9 \to \mathbb{R}^m$ being an activation function, and $\boldsymbol{W}_{\boldsymbol{\xi},i} \in \mathbb{R}^{m\times 9}$ and $\boldsymbol{W}_{\boldsymbol{X},i} \in \mathbb{R}^{m\times m}$ denote the input matrix and the internal matrix of the echo state network respectively.

Then, we can construct the following neural predictor for the kinetics (16)

$$\dot{\hat{\boldsymbol{\nu}}}_i = \boldsymbol{M}_i^{-1}\boldsymbol{\tau}_i + \boldsymbol{W}_i^{\mathrm{T}}\boldsymbol{X}_i - (\boldsymbol{K}_{i,2} + \boldsymbol{\rho}_i)(\hat{\boldsymbol{\nu}}_i - \boldsymbol{\nu}_i) \quad (18)$$

where $\hat{\boldsymbol{\nu}}_i \in \mathbb{R}^3$ denotes an estimation of $\boldsymbol{\nu}_i$, $\boldsymbol{K}_{i,2} \in \mathbb{R}^{3\times 3}$ is a positive definite control gain, and $\boldsymbol{\rho}_i \in \mathbb{R}^{3\times 3}$ denotes a tuning parameter matrix.

An adaptation law is designed for $\boldsymbol{W}_i^*$ by using a high-order tuner as follows

$$\begin{cases} \dot{\boldsymbol{\Theta}}_i = -\frac{\gamma_i}{\mathcal{T}_i}\boldsymbol{X}_i\boldsymbol{e}_i^{\mathrm{T}}(\hat{\boldsymbol{\nu}}_i, \boldsymbol{\nu}_i) \\ \dot{\boldsymbol{W}}_i = -\Gamma_i(\boldsymbol{W}_i - \boldsymbol{\Theta}_i) \end{cases} \quad (19)$$

where $\boldsymbol{e}_i(\hat{\boldsymbol{\nu}}_i, \boldsymbol{\nu}_i) = \dot{\tilde{\boldsymbol{\nu}}}_i + (\boldsymbol{K}_{i,2} + \boldsymbol{\rho}_i)\tilde{\boldsymbol{\nu}}_i$ with $\tilde{\boldsymbol{\nu}}_i = \hat{\boldsymbol{\nu}}_i - \boldsymbol{\nu}_i$, $\mathcal{T}_i = 1 + \|\boldsymbol{X}_i\|^2$, and $\gamma_i \in \mathbb{R}^+$ and $\Gamma_i \in \mathbb{R}^+$ are tuning parameters.

The dynamics of the subsystem consisting of $\tilde{\boldsymbol{\nu}}_i$, $\boldsymbol{\Theta}_i$, and $\boldsymbol{W}_i$ is given by the following form

$$\begin{cases} \dot{\tilde{\boldsymbol{\nu}}}_i = \tilde{\boldsymbol{W}}_i^{\mathrm{T}}\boldsymbol{X}_i - \boldsymbol{\varepsilon}_i - (\boldsymbol{K}_{i,2} + \boldsymbol{\rho}_i)\tilde{\boldsymbol{\nu}}_i \\ \dot{\boldsymbol{\Theta}}_i = -\frac{\gamma_i}{\mathcal{T}_i}\boldsymbol{X}_i\boldsymbol{e}_i^{\mathrm{T}}(\hat{\boldsymbol{\nu}}_i, \boldsymbol{\nu}_i) \\ \dot{\boldsymbol{W}}_i = -\Gamma_i(\boldsymbol{W}_i - \boldsymbol{\Theta}_i). \end{cases} \quad (20)$$

This article has been accepted for publication in IEEE Transactions on Intelligent Vehicles. This is the author's version which has not been fully edited and content may change prior to final publication. Citation information: DOI 10.1109/TIV.2022.3222009

where $\tilde{\boldsymbol{W}}_i = \boldsymbol{W}_i - \boldsymbol{W}_i^*$.

Remark 3. Echo state network is a class of recurrent neural networks. The hidden layer of the echo state network is sparsely connected. The connectivity and weights of hidden neurons are fixed and randomly assigned. Compared with the single-hidden neural network used in [43], the input weights of the echo state network are fixed, and the training of the input weights is not required. Compared with the fuzzy logic systems used in [14] and the RBF neural network used in [8], [10], [22], the echo state network has fewer tuning parameters. But, it should be noted that there is no significant difference in the approximation accuracy of these intelligent methods.

Remark 4. The meaning of acceleration considered herein is to speed up the convergence rate of the adaptive approximation. The convergence rate is a measure of how fast the difference between the solution point and its estimates goes to a minimum. Ref. [36], [37] developed a class of high-order tuner as the accelerated learning approach and also analyzed that the convergence rate of the high-order tuner-based adaptation is faster than the convergence rate of the gradient descent-based adaptation for discrete systems. Based on this merit, an accelerated learning-based neural predictor is designed for ISVs by using the high-order tuner.

C. Cooperative maneuvering controllers based on Nash equilibrium seeking

In this subsection, based on the previous action estimators and accelerated learning-based neural predictors, a controller is designed for the ith ISV by using a Nash equilibrium seeking approach, consisting of a kinematic control law, a kinetic control law, and an update law for the individual parameter.

Step 1. Define a kinematic error $\boldsymbol{z}_{i,1} = \boldsymbol{R}^{\mathrm{T}}(\psi_i)(\boldsymbol{\eta}_i - \bar{\boldsymbol{\eta}}_i)$, where

$$\dot{\bar{\boldsymbol{\eta}}}_i = \boldsymbol{\delta}_{\eta,i} g_{i,1}(\hat{\boldsymbol{\eta}}) \tag{21}$$

is a Nash equilibrium seeking strategy with $\boldsymbol{\delta}_{\eta,i} \in \mathbb{R}^{3\times 3}$ being a gain matrix. The dynamics of $\boldsymbol{z}_{i,1}$ is given by

$$\dot{\boldsymbol{z}}_{i,1} = \dot{\boldsymbol{R}}^{\mathrm{T}}(\psi_i)(\boldsymbol{\eta}_i - \bar{\boldsymbol{\eta}}_i) + \boldsymbol{\nu}_i - \boldsymbol{R}^{\mathrm{T}}(\psi_i)\dot{\bar{\boldsymbol{\eta}}}_i. \tag{22}$$

To stabilize (22), the following kinematic control law can be constructed as follows

$$\boldsymbol{\alpha}_i = -\boldsymbol{K}_{i,1}\boldsymbol{z}_{i,1} - \dot{\boldsymbol{R}}^{\mathrm{T}}(\psi_i)(\boldsymbol{\eta}_i - \bar{\boldsymbol{\eta}}_i) + \boldsymbol{R}^{\mathrm{T}}(\psi_i)\dot{\bar{\boldsymbol{\eta}}}_i \tag{23}$$

where $\boldsymbol{K}_{i,1} = \mathrm{diag}\{k_{x,i}, k_{y,i}, k_{\psi,i}\} \in \mathbb{R}^{3\times 3}$ with $k_{x,i} \in \mathbb{R}^+$, $k_{y,i} \in \mathbb{R}^+$, and $k_{\psi,i} \in \mathbb{R}^+$ being control gains.

Define $\boldsymbol{\alpha}_{\mathrm{f},i} \in \mathbb{R}^3$ as an estimated signal of $\boldsymbol{\alpha}_i$ and $\boldsymbol{\alpha}_{\mathrm{f},i}^{\mathrm{d}} \in \mathbb{R}^3$ as an estimated signal of $\dot{\boldsymbol{\alpha}}_i$, a nonlinear command filter is introduced as follows [44]

$$\begin{cases} \dot{\boldsymbol{\alpha}}_{\mathrm{f},i} = -\boldsymbol{\zeta}_{i,1}\mathrm{sig}^{\frac{1}{2}}(\boldsymbol{\alpha}_{\mathrm{f},i} - \boldsymbol{\alpha}_i) + \boldsymbol{\alpha}_{\mathrm{f},i}^{\mathrm{d}} \\ \dot{\boldsymbol{\alpha}}_{\mathrm{f},i}^{\mathrm{d}} = -\boldsymbol{\zeta}_{i,2}\mathrm{sig}^{0}(\boldsymbol{\alpha}_{\mathrm{f},i}^{\mathrm{d}} - \dot{\boldsymbol{\alpha}}_{\mathrm{f},i}) \end{cases} \tag{24}$$

where $\boldsymbol{\zeta}_{i,1} \in \mathbb{R}^{3\times 3}$ and $\boldsymbol{\zeta}_{i,2} \in \mathbb{R}^{3\times 3}$ are the positive definite diagonal coefficient matrices. According to the stability conclusion in [44], the command filter (24) is finite-time stable and satisfying $\|\boldsymbol{\alpha}_{\mathrm{f},i} - \boldsymbol{\alpha}_i\| \le \bar{\alpha}_i \in \mathbb{R}^+$ and $\|\boldsymbol{\alpha}_{\mathrm{f},i}^{\mathrm{d}} - \dot{\boldsymbol{\alpha}}_i\| \le \bar{\alpha}_i^{\mathrm{d}} \in \mathbb{R}^+$.

Step 2. Define a kinetic error $\hat{\boldsymbol{z}}_{i,2} = \boldsymbol{\nu}_i - \boldsymbol{\alpha}_{\mathrm{f},i}$, and the dynamics of $\hat{\boldsymbol{z}}_{i,2}$ is given by

$$\dot{\hat{\boldsymbol{z}}}_{i,2} = \boldsymbol{M}_i^{-1}\boldsymbol{\tau}_i + \boldsymbol{W}_i^{\mathrm{T}}\boldsymbol{X}_i - (\boldsymbol{K}_{i,2} + \boldsymbol{\rho}_i)\tilde{\boldsymbol{\nu}}_i - \boldsymbol{\alpha}_{\mathrm{f},i}^{\mathrm{d}}. \tag{25}$$

To stabilize (25) and the total closed-loop system, the following kinetic control law is chosen as follows

$$\boldsymbol{u}_i = \boldsymbol{M}_i(-\boldsymbol{K}_{i,2}\boldsymbol{z}_{i,2} - \boldsymbol{W}_i^{\mathrm{T}}\boldsymbol{X}_i + \boldsymbol{\alpha}_{\mathrm{f},i}^{\mathrm{d}}) - \boldsymbol{z}_{i,1} \tag{26}$$

where $\boldsymbol{K}_{i,2} = \mathrm{diag}\{k_{u,i}, k_{v,i}, k_{r,i}\} \in \mathbb{R}^{3\times 3}$ with $k_{u,i} \in \mathbb{R}^+$, $k_{v,i} \in \mathbb{R}^+$, and $k_{r,i} \in \mathbb{R}^+$ being control gains.

Step 3. Define a parameter error $z_{i,3} = \theta_i - \bar{\theta}_i$, where

$$\dot{\bar{\theta}}_i = \delta_{\theta,i} g_{i,2}(\hat{\boldsymbol{\theta}}) \tag{27}$$

is a Nash equilibrium seeking strategy with $\delta_{\theta,i} \in \mathbb{R}^+$ being a gain. Then, a parameter update law $\tau_{\mathrm{p},i}$ is designed as follows

$$\tau_{\mathrm{p},i} = -k_{i,3}z_{i,3} + \dot{\bar{\theta}}_i. \tag{28}$$

At last, the dynamics of the subsystem with respect to $\boldsymbol{z}_{i,1}$, $\hat{\boldsymbol{z}}_{i,2}$, and $z_{i,3}$ is given as follows

$$\begin{cases} \dot{\boldsymbol{z}}_{i,1} = -\boldsymbol{K}_{i,1}\boldsymbol{z}_{i,1} + \hat{\boldsymbol{z}}_{i,2} - \tilde{\boldsymbol{\nu}}_i + \boldsymbol{\iota}_i \\ \dot{\hat{\boldsymbol{z}}}_{i,2} = -\boldsymbol{K}_{i,2}\hat{\boldsymbol{z}}_{i,2} - \boldsymbol{z}_{i,1} - \boldsymbol{\rho}_i\tilde{\boldsymbol{\nu}}_i \\ \dot{z}_{i,3} = -k_{i,3}z_{i,3} \end{cases} \tag{29}$$

where $\boldsymbol{\iota}_i = \boldsymbol{\alpha}_{\mathrm{f},i} - \boldsymbol{\alpha}_i$.

IV. Main Results

In the previous section, distributed cooperative maneuvering controllers have been designed based on the Nash equilibrium seeking strategy for multiple ISVs. In this section, the stability of the closed-loop system is established. The following theorem can be concluded.

Theorem 1. Consider the distributed noncooperative game (3) and (5) played by multiple ISVs with the kinematics (1) and kinetics (2). The proposed Nash equilibrium seeking strategy-based controller is chosen for cooperative maneuvering as action estimators (9) and (10), neural predictors based on the accelerated learning (18) and (19), kinematic control laws (23), kinetic control laws (26), and parameter update laws (28). If *Assumptions 1-3* hold, (i) all subsystems are input-to-state stable; (ii) the total closed-loop system is input-to-state stable. (iii) *Geometric Task* and *Dynamic Task* of noncooperative game-based cooperative maneuvering can be achieved.

Proof: At first, we consider the input-to-state stability of the subsystem governed by (15). Define the following candidate Lyapunov function for the subsystem (15)

$$V_{i,\mathrm{p}} = \frac{1}{2}\tilde{\boldsymbol{\nu}}_i^{\mathrm{T}}\tilde{\boldsymbol{\nu}}_i + \frac{1}{\gamma_i}\|\boldsymbol{\Theta}_i - \boldsymbol{W}_i^*\|_{\mathrm{F}}^2 + \frac{1}{\gamma_i}\|\boldsymbol{\Theta}_i - \boldsymbol{W}_i\|_{\mathrm{F}}^2$$

and its time derivative along (15) is taken as

$$\begin{aligned} \dot{V}_{i,\mathrm{p}} =& \tilde{\boldsymbol{\nu}}_i^{\mathrm{T}}[\tilde{\boldsymbol{W}}_i^{\mathrm{T}}\boldsymbol{X}_i - \boldsymbol{\varepsilon}_i - (\boldsymbol{K}_{i,2} + \boldsymbol{\rho}_i)\tilde{\boldsymbol{\nu}}_i] \\ &+ \frac{2}{\gamma_i}\mathrm{tr}([\boldsymbol{\Theta}_i - \boldsymbol{W}_i + \tilde{\boldsymbol{W}}_i]^{\mathrm{T}}[-\frac{\gamma_i}{\mathcal{T}_i}\boldsymbol{X}_i\boldsymbol{e}_i^{\mathrm{T}}(\hat{\boldsymbol{\nu}}_i, \boldsymbol{\nu}_i)]) \\ &+ \frac{2}{\gamma_i}\mathrm{tr}([\boldsymbol{\Theta}_i - \boldsymbol{W}_i]^{\mathrm{T}}[-\frac{\gamma_i}{\mathcal{T}_i}\boldsymbol{X}_i\boldsymbol{e}_i^{\mathrm{T}}(\hat{\boldsymbol{\nu}}_i, \boldsymbol{\nu}_i) \\ &+ \Gamma_i(\boldsymbol{W}_i - \boldsymbol{\Theta}_i)]) \end{aligned}$$

This article has been accepted for publication in IEEE Transactions on Intelligent Vehicles. This is the author's version which has not been fully edited and content may change prior to final publication. Citation information: DOI 10.1109/TIV.2022.3222009

It follows that

$$\begin{aligned}\dot{V}_{i,\mathrm{p}} =&\tilde{\boldsymbol{\nu}}_i^{\mathrm{T}}[\boldsymbol{e}_i-(\boldsymbol{K}_{i,2}+\boldsymbol{\rho}_i)\tilde{\boldsymbol{\nu}}_i]\\&+\frac{1}{\mathcal{T}_i}\{-2\boldsymbol{e}_i^{\mathrm{T}}\boldsymbol{e}_i-2\frac{\Gamma_i}{\gamma_i}\mathrm{tr}([\boldsymbol{W}_i-\boldsymbol{\Theta}_i]^{\mathrm{T}}[\boldsymbol{W}_i-\boldsymbol{\Theta}_i])\\&-2\frac{\Gamma_i}{\gamma_i}\|\boldsymbol{X}_i\|^2\mathrm{tr}([\boldsymbol{W}_i-\boldsymbol{\Theta}_i]^{\mathrm{T}}[\boldsymbol{W}_i-\boldsymbol{\Theta}_i])\\&+4\mathrm{tr}([\boldsymbol{W}_i-\boldsymbol{\Theta}_i]^{\mathrm{T}}\boldsymbol{X}_i\boldsymbol{e}_i^{\mathrm{T}})\}\end{aligned}\tag{30}$$

When $\Gamma_i \geq 2\gamma_i$, Eq. (30) can be further put into

$$\begin{aligned}\dot{V}_{i,\mathrm{p}} \leq&-\lambda_{\min}(\boldsymbol{K}_{i,2}+\boldsymbol{\rho}_i)\|\tilde{\boldsymbol{\nu}}_i\|^2+\|\tilde{\boldsymbol{\nu}}_i\|\|\boldsymbol{e}_i\|\\&+\frac{1}{\mathcal{T}_i}\{-\frac{2\Gamma_i}{\gamma_i}\|\boldsymbol{W}_i-\boldsymbol{\Theta}_i\|_{\mathrm{F}}^2-\|\boldsymbol{e}_i\|^2-[\|\boldsymbol{e}_i\|\\&-2\|\boldsymbol{W}_i-\boldsymbol{\Theta}_i\|_{\mathrm{F}}\|\boldsymbol{X}_i\|]^2\}\end{aligned}$$

Then, one has

$$\begin{aligned}\dot{V}_{i,\mathrm{p}} \leq&-\lambda_{\min}(\boldsymbol{K}_{i,2}+\boldsymbol{\rho}_i)\|\tilde{\boldsymbol{\nu}}_i\|^2-\frac{2\Gamma_i}{\gamma_i\mathcal{T}_i}\|\boldsymbol{W}_i-\boldsymbol{\Theta}_i\|_{\mathrm{F}}^2\\&+\|\tilde{\boldsymbol{\nu}}_i\|\|\boldsymbol{e}_i\|\\\leq&-c_{i,1}\|\boldsymbol{E}_i\|^2+\|\boldsymbol{E}_i\|\|\boldsymbol{e}_i\|\end{aligned}$$

where $c_{i,1}=\min\{\lambda_{\min}(\boldsymbol{K}_{i,2}+\boldsymbol{\rho}_i),2\Gamma_i/\gamma_i\mathcal{T}_i\}$ and $\boldsymbol{E}_i=[\|\tilde{\boldsymbol{\nu}}_i\|,\|\boldsymbol{W}_i-\boldsymbol{\Theta}_i\|_{\mathrm{F}}]^{\mathrm{T}}$.

Since $\|\boldsymbol{E}_i\|\geq 2\|\boldsymbol{e}_i\|/c_{i,1}$ makes $\dot{V}_{i,\mathrm{p}}\leq -c_{i,1}\|\boldsymbol{E}_i\|^2/2$, the subsystem (15) is input-to-state stable. Moreover for all $t>t_0$, $\|\boldsymbol{E}_i(t_0)\|$ satisfies

$$\|\boldsymbol{E}_i(t_0)\|\leq\Upsilon_{i,\boldsymbol{E}_i}(\boldsymbol{E}_i(t),t-t_0)+g_{\boldsymbol{e}_i}(\|\boldsymbol{e}_i\|)$$

where $\Upsilon_{i,\boldsymbol{E}_i}(\cdot)$ is a class $\mathcal{KL}$ function, and $g_{\boldsymbol{e}_i}(s)=2\sqrt{\lambda_{\max}(\boldsymbol{P}_{i,\mathrm{p}})}s/c_{i,1}\sqrt{\lambda_{\max}(\boldsymbol{P}_{i,\mathrm{p}})}$ with $\boldsymbol{P}_{i,\mathrm{p}}=\mathrm{diag}\{1,2/\gamma_i\}$.

Then, we consider the input-to-state stability of the subsystem governed by (29). Define the following candidate Lyapunov function for the subsystem (29)

$$V_{\mathrm{c}}=\sum_{i=1}^{M}\left(\frac{1}{2}\boldsymbol{z}_{i,1}^{\mathrm{T}}\boldsymbol{z}_{i,1}+\frac{1}{2}\hat{\boldsymbol{z}}_{i,2}^{\mathrm{T}}\hat{\boldsymbol{z}}_{i,2}+\frac{1}{2}z_{i,3}^2\right)$$

and its time derivative along (29) is taken as

$$\begin{aligned}\dot{V}_c=\sum_{i=1}^{M}\Big(&-\boldsymbol{z}_{i,1}^{\mathrm{T}}\boldsymbol{K}_{i,1}\boldsymbol{z}_{i,1}-\boldsymbol{z}_{i,1}^{\mathrm{T}}\tilde{\boldsymbol{\nu}}_i+\boldsymbol{z}_{i,1}^{\mathrm{T}}\boldsymbol{\iota}_i\\&-\hat{\boldsymbol{z}}_{i,2}^{\mathrm{T}}\boldsymbol{K}_{i,2}\hat{\boldsymbol{z}}_{i,2}-\boldsymbol{z}_{i,2}^{\mathrm{T}}\boldsymbol{\rho}_i\tilde{\boldsymbol{\nu}}_i-k_{i,3}z_{i,3}^2\Big).\end{aligned}$$

Letting $\boldsymbol{Z}=[\boldsymbol{Z}_1^{\mathrm{T}},...,\boldsymbol{Z}_1^{\mathrm{T}}]^{\mathrm{T}}$ with $\boldsymbol{Z}_i^{\mathrm{T}}=[\boldsymbol{z}_{i,1}^{\mathrm{T}},\hat{\boldsymbol{z}}_{i,2}^{\mathrm{T}},z_{i,3}]^{\mathrm{T}}$, it follows that

$$\begin{aligned}\dot{V}_c\leq&-c_2\|\boldsymbol{Z}\|^2+\|\boldsymbol{Z}\|\sum_{i=1}^{M}\Big((\lambda_{\max}(\boldsymbol{\rho}_i)+1)\|\tilde{\boldsymbol{\nu}}_i\|+\|\boldsymbol{\iota}_i\|\Big)\\\leq&-c_2\|\boldsymbol{Z}\|^2+\|\boldsymbol{Z}\|\sum_{i=1}^{M}\|\boldsymbol{U}_i\|\end{aligned}$$

where $c_2=\min_{i=1}^{M}\{\lambda_{\min}(\boldsymbol{K}_{i,1}),\lambda_{\min}(\boldsymbol{K}_{i,2})\}$ and $\boldsymbol{U}_i=[(\lambda_{\max}(\boldsymbol{\rho}_i)+1)\|\tilde{\boldsymbol{\nu}}_i\|,\|\boldsymbol{\iota}_i\|]^{\mathrm{T}}$.

Since $\|\boldsymbol{Z}\|\geq 2\|\boldsymbol{U}_i\|/c_2$ makes $\dot{V}_c\leq -c_2\|\boldsymbol{Z}\|^2/2$, the subsystem (29) is input-to-state stable. Moreover for all $t>t_0$, $\|\boldsymbol{Z}(t_0)\|$ satisfies

$$\begin{aligned}\|\boldsymbol{Z}(t_0)\|\leq&\Upsilon_{\boldsymbol{Z}}(\boldsymbol{Z}(t),t-t_0)\\&+\sum_{i=1}^{M}\left(g_{\tilde{\boldsymbol{\nu}}_i}(\|\tilde{\boldsymbol{\nu}}_i\|)+g_{\boldsymbol{\iota}_i}(\|\tilde{\boldsymbol{\iota}}_i\|)\right)\end{aligned}$$

where $\Upsilon_{\boldsymbol{Z}}(\cdot)$ is a class $\mathcal{KL}$ function, $g_{\tilde{\boldsymbol{\nu}}_i}(s)=2((\lambda_{\max}(\boldsymbol{\rho}_i)+1))s/c_2$, and $g_{\boldsymbol{\iota}_i}(s)=2s/c_2$.

Then, we consider the input-to-state stability of the subsystem governed by (15). Define the following candidate Lyapunov function

$$V_{\mathrm{a}}=\tilde{\boldsymbol{\eta}}^{\mathrm{T}}\bar{\boldsymbol{H}}\tilde{\boldsymbol{\eta}}+\tilde{\boldsymbol{\theta}}^{\mathrm{T}}\boldsymbol{H}\tilde{\boldsymbol{\theta}}$$

where $\bar{\boldsymbol{H}}=\boldsymbol{H}\otimes\boldsymbol{I}_3$. Its time derivative along (15) is taken as

$$\begin{aligned}\dot{V}_a=&-\tilde{\boldsymbol{\eta}}^{\mathrm{T}}\bar{\boldsymbol{H}}\boldsymbol{\mu}\bar{\boldsymbol{H}}\tilde{\boldsymbol{\eta}}+\tilde{\boldsymbol{\eta}}^{\mathrm{T}}\bar{\boldsymbol{H}}(\boldsymbol{1}_M\otimes\boldsymbol{K}_1\boldsymbol{z}_1)-\tilde{\boldsymbol{\eta}}^{\mathrm{T}}\bar{\boldsymbol{H}}(\boldsymbol{1}_M\otimes\hat{\boldsymbol{z}}_2)\\&+\tilde{\boldsymbol{\eta}}^{\mathrm{T}}\bar{\boldsymbol{H}}(\boldsymbol{1}_M\otimes\tilde{\boldsymbol{\nu}})-\tilde{\boldsymbol{\eta}}^{\mathrm{T}}\bar{\boldsymbol{H}}(\boldsymbol{1}_M\otimes\boldsymbol{\iota})\\&-\tilde{\boldsymbol{\eta}}^{\mathrm{T}}\bar{\boldsymbol{H}}(\boldsymbol{1}_M\otimes\boldsymbol{\delta}_\eta\boldsymbol{g}_\eta(\hat{\boldsymbol{\eta}}))-\tilde{\boldsymbol{\theta}}^{\mathrm{T}}\boldsymbol{H}\boldsymbol{\kappa}\boldsymbol{H}\tilde{\boldsymbol{\theta}}\\&+\tilde{\boldsymbol{\theta}}^{\mathrm{T}}\boldsymbol{H}(\boldsymbol{1}_M\otimes\boldsymbol{k}_3\boldsymbol{z}_3)-\tilde{\boldsymbol{\theta}}^{\mathrm{T}}\boldsymbol{H}(\boldsymbol{1}_M\otimes\boldsymbol{\delta}_\theta\boldsymbol{g}_\theta(\hat{\boldsymbol{\theta}}))\end{aligned}$$

with $\boldsymbol{z}_1=[\boldsymbol{z}_{1,1}^{\mathrm{T}},...,\boldsymbol{z}_{M,1}^{\mathrm{T}}]^{\mathrm{T}}\in\mathbb{R}^{3M}$, $\hat{\boldsymbol{z}}_2=[\hat{\boldsymbol{z}}_{1,2}^{\mathrm{T}},...,\hat{\boldsymbol{z}}_{M,2}^{\mathrm{T}}]^{\mathrm{T}}\in\mathbb{R}^{3M}$, $z_3=[z_{1,3},...,z_{M,3}]^{\mathrm{T}}\in\mathbb{R}^{M}$, $\tilde{\boldsymbol{\nu}}=[\tilde{\boldsymbol{\nu}}_1^{\mathrm{T}},...,\tilde{\boldsymbol{\nu}}_M^{\mathrm{T}}]^{\mathrm{T}}\in\mathbb{R}^{3M}$, $\boldsymbol{\iota}=[\boldsymbol{\iota}_1^{\mathrm{T}},...,\boldsymbol{\iota}_M^{\mathrm{T}}]^{\mathrm{T}}\in\mathbb{R}^{3M}$, $\boldsymbol{g}_\eta(\hat{\boldsymbol{\eta}})=[\boldsymbol{g}_{1,1}^{\mathrm{T}}(\hat{\boldsymbol{\eta}}),...,\boldsymbol{g}_{M,1}^{\mathrm{T}}(\hat{\boldsymbol{\eta}})]^{\mathrm{T}}\in\mathbb{R}^{3M}$, $\boldsymbol{g}_\eta(\hat{\boldsymbol{\theta}})=[g_{1,2}^{\mathrm{T}}(\hat{\boldsymbol{\theta}}),...,g_{M,2}^{\mathrm{T}}(\hat{\boldsymbol{\theta}})]^{\mathrm{T}}\in\mathbb{R}^{M}$, $\boldsymbol{K}_1=\mathrm{diag}\{\boldsymbol{K}_{1,1},...,\boldsymbol{K}_{M,1}\}\in\mathbb{R}^{3M\times 3M}$, $\boldsymbol{k}_3=\mathrm{diag}\{k_{1,3},...,k_{M,3}\}\in\mathbb{R}^{M\times M}$, $\boldsymbol{\delta}_\eta=\mathrm{diag}\{\boldsymbol{\delta}_{\eta,1},...,\boldsymbol{\delta}_{\eta,M}\}\in\mathbb{R}^{3M\times 3M}$, $\boldsymbol{\delta}_\theta=\mathrm{diag}\{\delta_{\theta,1},...,\delta_{\theta,M}\}\in\mathbb{R}^{M\times M}$.

Define $\varrho_1,\varrho_2,\varrho_3,\varrho_4\in\mathbb{R}^+$, and we can obtain

$$\begin{aligned}\dot{V}_a\leq&-c_3\|\tilde{\boldsymbol{\eta}}\|^2-c_4\|\tilde{\boldsymbol{\theta}}\|^2\\&+M\lambda_{\max}(\bar{\boldsymbol{H}})(\lambda_{\max}(\boldsymbol{K}_1)+\varrho_3\lambda_{\max}(\boldsymbol{\delta}_\eta))\|\tilde{\boldsymbol{\eta}}\|\|\boldsymbol{z}_1\|\\&+M\lambda_{\max}(\bar{\boldsymbol{H}})\|\tilde{\boldsymbol{\eta}}\|\|\hat{\boldsymbol{z}}_2\|+M\lambda_{\max}(\bar{\boldsymbol{H}})\|\tilde{\boldsymbol{\eta}}\|\|\boldsymbol{\iota}\|\\&+M\lambda_{\max}(\boldsymbol{H})(\lambda_{\max}(\boldsymbol{k}_3)+\varrho_4\lambda_{\max}(\boldsymbol{\delta}_\theta))\|\tilde{\boldsymbol{\theta}}\|\|\boldsymbol{z}_3\|\\\leq&-c_5\|\boldsymbol{E}_a\|^2+Mc_6\|\boldsymbol{E}_a\|\|\boldsymbol{Z}\|+M\lambda_{\max}(\bar{\boldsymbol{H}})\|\boldsymbol{E}_a\|\|\boldsymbol{\iota}\|\end{aligned}$$

where $c_3=(\lambda_{\min}(\boldsymbol{\mu})\lambda_{\min}^2(\bar{\boldsymbol{H}})-M\varrho_1\lambda_{\max}(\boldsymbol{\delta}_\eta)))$, $c_4=(\lambda_{\min}(\boldsymbol{\kappa})\lambda_{\min}^2(\boldsymbol{H})-M\varrho_2\lambda_{\max}(\boldsymbol{\delta}_\theta)))$ $\boldsymbol{E}_a=[\|\tilde{\boldsymbol{\eta}}\|,\|\tilde{\boldsymbol{\theta}}\|]^{\mathrm{T}}$, $c_5=\min\{c_3,c_4\}$, $c_6=\max\{\lambda_{\max}(\bar{\boldsymbol{H}})(\lambda_{\max}(\boldsymbol{K}_1)+\varrho_3\lambda_{\max}(\boldsymbol{\delta}_\eta)),\lambda_{\max}(\boldsymbol{H})(\lambda_{\max}(\boldsymbol{k}_3)+\varrho_4\lambda_{\max}(\boldsymbol{\delta}_\theta)),\lambda_{\max}(\bar{\boldsymbol{H}})\}$

Since $\|\boldsymbol{E}_a\|\geq 2M(c_6\|\boldsymbol{Z}\|+\lambda_{\max}(\bar{\boldsymbol{H}})\|\boldsymbol{\iota}\|)/c_5$ makes $\dot{V}_a\leq -c_5\|\boldsymbol{E}_a\|^2/2$, the subsystem (15) is input-to-state stable. Moreover for all $t>t_0$, $\|\boldsymbol{E}_a(t_0)\|$ satisfies

$$\begin{aligned}\|\boldsymbol{E}_a(t_0)\|\leq&\Upsilon_{\boldsymbol{E}_a}(\boldsymbol{E}_a(t),t-t_0)\\&+M\left(g_{\boldsymbol{Z}}(\|\boldsymbol{Z}\|)+g_{\boldsymbol{\iota}}(\|\boldsymbol{\iota}\|)\right)\end{aligned}$$

where $\Upsilon_{\boldsymbol{E}_a}(\cdot)$ is a class $\mathcal{KL}$ function, $g_{\boldsymbol{Z}}(s)=2\sqrt{\lambda_{\max}(\boldsymbol{P}_a)}c_6s/\sqrt{\lambda_{\min}(\boldsymbol{P}_a)}c_5$, $g_{\boldsymbol{\iota}}(s)=2\sqrt{\lambda_{\max}(\boldsymbol{P}_{\mathrm{a}})}\lambda_{\max}(\bar{\boldsymbol{H}})s/\sqrt{\lambda_{\min}(\boldsymbol{P}_{\mathrm{a}})}c_5$, and $\boldsymbol{P}_{\mathrm{a}}=\mathrm{diag}\{\bar{\boldsymbol{H}},\boldsymbol{H}\}$.

The above three subsystems are proved to be input-to-state stable. For the subsystem governed by (29), an input $\tilde{\boldsymbol{\nu}}_i$ is a state of the subsystem governed by (20). For the subsystem governed by (15), an input $\boldsymbol{Z}$ is a state of the subsystem

governed by (29). Therefore, the resulting closed-loop system can be regarded as a system cascaded by these subsystems. By using *Lemma C.4* in [45], the input-to-state stability of the total closed-loop system can be established.

Ref. [29] has proved that $\bar{\boldsymbol{\eta}}_i$ can converge to $\boldsymbol{\eta}_i^*$ under the Nash equilibrium seeking strategy (21) and $\bar{\theta}_i$ can converge to θ_i^* under the Nash equilibrium seeking strategy (27). Because the total closed-loop system is input-to-state stable, $\boldsymbol{z}_{i,1}$ and $z_{i,3}$ are ultimately bounded. It follows that $\|\boldsymbol{\eta}_i - \boldsymbol{\eta}_i^*\|$ and $|\theta_i - \theta_i^*|$ are ultimately bounded. Therefore, for cooperative maneuvering, *Geometric Task* governed by (3) and *Dynamic Task* governed by (5) can be achieved. ■

Remark 5. Input-to-state stability is chosen as the analysis tool to simplify the analysis complexity by dividing the total closed-loop system into several simple subsystems. The total closed-loop system is input-to-state stable by using the cascade stability theory (*Lemma C.4* in [45]) as long as these subsystems are input-to-state stable. There exists a connection between the Lyapunov analysis-based boundedness and the input-to-state stability. Consider a system $\dot{x} = f(x,u)$. The input-to-state stability of $\dot{x} = f(x,u)$ implies that $x(t)$ is ultimate bounded by $\kappa(\sup(\|x(\tau)\|))$ where $\tau \in (t, t_0)$ and $\kappa(\cdot)$ is a class $\mathcal{K}$ function. In [46], the Lyapunov-like theorem that follows gives a sufficient condition for input-to-state stability, see *Theorem 4.6* in [46]. This theorem means we can use a Lyapunov-like analysis to establish the input-to-state stability of the total closed-loop system.

V. An Application with Simulation Results

To demonstrate the effectiveness of the proposed distributed Nash equilibrium seeking-based controllers for noncooperative game-based cooperative maneuvering of multiple ISVs, a simulation example is presented. Consider a distributed noncooperative game of 5 ISVs, labeled as $1-5$, where the communication topology is described in Fig. 2. The model parameters of ISVs considered herein can be found in [47]. The considered distributed cooperative maneuvering occurs in the part of Yangcheng Lake, China.

The first payoff function $J_{i,1}(\boldsymbol{\eta}, \boldsymbol{\eta}_{\mathrm{r},i}(\theta_i))$ of the ith ISV with respect to *Geometric Task* is

$$\begin{aligned} J_{i,1}(\boldsymbol{\eta}, \boldsymbol{\eta}_{\mathrm{r},i}(\theta_i)) =& (x_i - x_{\mathrm{r},i}(\theta_i))^2 + (y_i - y_{\mathrm{r},i}(\theta_i))^2 \\ &+ (\psi_i - \psi_{\mathrm{r},i}(\theta_i))^2 - (0.1\sum_{k=1}^{5} x_k \\ &+ 100\cos(\theta_i))x_i - (0.1\sum_{k=1}^{5} y_k \\ &+ 100\sin(\theta_i))y_i - (0.01\sum_{k=1}^{5} \psi_k)\psi_i \end{aligned} \tag{31}$$

where $\boldsymbol{\eta}_{\mathrm{r},i}(\theta_i) = [x_{\mathrm{r},i}(\theta_i), y_{\mathrm{r},i}(\theta_i), \psi_{\mathrm{r},i}(\theta_i)]^{\mathrm{T}}$, $x_{\mathrm{r},1}(\theta_1) = 150\cos(\theta_1)$, $x_{\mathrm{r},2}(\theta_2) = 170\cos(\theta_1)$, $x_{\mathrm{r},3}(\theta_3) = 190\cos(\theta_1)$, $x_{\mathrm{r},4}(\theta_4) = 210\cos(\theta_4)$, $x_{\mathrm{r},5}(\theta_5) = 230\cos(\theta_5)$, $y_{\mathrm{r},1}(\theta_1) = 150\sin(\theta_1)$, $y_{\mathrm{r},2}(\theta_2) = 170\sin(\theta_2)$, $y_{\mathrm{r},3}(\theta_3) = 190\sin(\theta_3)$, $y_{\mathrm{r},4}(\theta_4) = 210\sin(\theta_1)$, $y_{\mathrm{r},5}(\theta_5) = 230\sin(\theta_5)$, $\psi_{\mathrm{r},i}(\theta_i) = 1.03\theta_i + 0.4855\pi$ with $i = 1, ..., 5$.

The second payoff function $J_{i,2}(\boldsymbol{\theta})$ of the ith ISV with respect to *Dynamic Task* is

$$J_{i,2}(\boldsymbol{\theta}) = (\theta_i - \theta_{\mathrm{r},i})^2 - (0.01\sum_{k=1}^{5} \theta_k)\theta_i \tag{32}$$

where $\theta_{\mathrm{r},i} = 0.0103t$ with $i = 1, ..., 5$. ISVs will achieve a formation influenced by $J_{i,1}(\cdot)$ and $J_{i,2}(\cdot)$. It should be noted that the proposed distributed Nash equilibrium seeking-based controllers for noncooperative game-based cooperative maneuvering can also perform these different tasks by utilizing the different payoff functions.

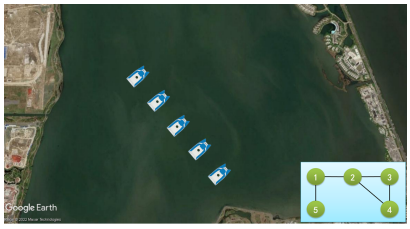

Fig. 2: An application with the communication topology (The underlaying map is from Google Earth.)

For the simulation, the parameters are selected as follows: $\boldsymbol{\mu}_{i,j} = \mathrm{diag}\{1,1,1\}$, $\kappa_{i,j} = 1$, $k_{x,i} = k_{y,i} = k_{\psi,i} = 0.2$, $k_{u,i} = k_{v,i} = k_{r,i} = 5$, $\boldsymbol{\rho}_i = \mathrm{diag}\{205, 205, 205\}$, $\gamma_i = 100$, $\Gamma_i = 200$, $\boldsymbol{\zeta}_{i,1} = \mathrm{diag}\{40, 40, 40\}$, $\boldsymbol{\zeta}_{i,2} = \mathrm{diag}\{0.05, 0.05, 0.05\}$, $\boldsymbol{\delta}_{\eta,i} = \mathrm{diag}\{1,1,1\}$, $\delta_{\theta,i} = 1$.

Figs. 3-8 show the simulation results of ISVs formation based on the proposed distributed Nash equilibrium seeking method. Fig. 3 depicts the actual trajectories of ISVs, and it can be seen that 5 ISVs are coordinated steering along the Nash equilibrium solution. Figs. 4-6 depict the revolution of the actual action $\boldsymbol{\eta}_i$ and the Nash equilibrium solutions $\boldsymbol{\eta}_i^*$, where $\boldsymbol{\eta}_i^* = [x_i^*, y_i^*, \psi_i^*]^{\mathrm{T}}$. It can be observed in Figs 4-6 that the actual action $\boldsymbol{\eta}_i$ can seek the Nash equilibrium $\boldsymbol{\eta}_i^*$, and thus *Geometric Task* is achieved. In Fig. 7, the evolution of the player parameter θ_i is depicted. 5 player parameters are coordinated such that *Dynamic Task* is achieved. In Fig. 8, the learning profile of echo state network is shown. It can be observed that the uncertain nonlinear term $\boldsymbol{F}_2(\cdot)$ can be estimated by using the proposed accelerated learning-based neural predictor.

The proposed accelerated learning-based neural predictor is also to compare with the existing neural predictor developed in [15]–[17] with the same adaptation gain to show the efficacy. The dynamics of neural predictor is given as follows

$$\begin{cases} \dot{\hat{\boldsymbol{\nu}}}_i = \boldsymbol{M}_i^{-1}\boldsymbol{\tau}_i + \boldsymbol{W}_i^{\mathrm{T}}\boldsymbol{X}_i - (\boldsymbol{K}_{i,2} + \boldsymbol{\rho}_i)\tilde{\boldsymbol{\nu}}_i \\ \dot{\boldsymbol{W}}_i = -\Gamma_i(\boldsymbol{X}_i\tilde{\boldsymbol{\nu}}_i^{\mathrm{T}} + \boldsymbol{\lambda}_i\boldsymbol{W}_i). \end{cases}$$

In Fig. 9, the comparison between the proposed accelerated learning-based neural predictor and the neural predictor is shown. Though these two methods can identify the uncertain nonlinearities terms, the proposed accelerated learning-based neural predictor has a faster convergence rate. It means that the high-order tuner can speed up the convergence rate of the gradient descent adaptation.

This article has been accepted for publication in IEEE Transactions on Intelligent Vehicles. This is the author's version which has not been fully edited and content may change prior to final publication. Citation information: DOI 10.1109/TIV.2022.3222009

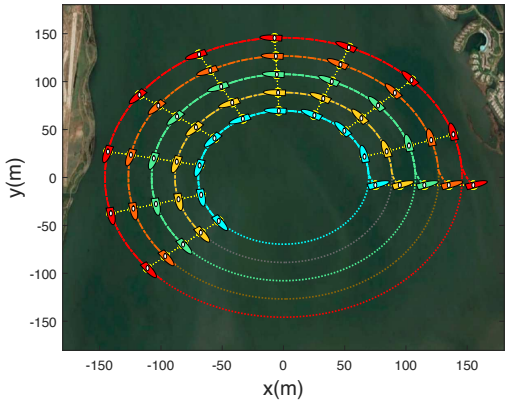

Fig. 3: The actual trajectories of 5 ISVs (dot dash line:actual trajectories; dotted line: Nash equilibrium solutions)

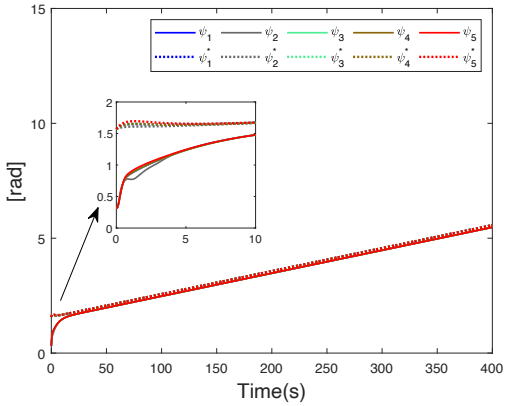

Fig. 6: Revolution of heading angles ψ_i and Nash equilibrium solutions ψ_i^*

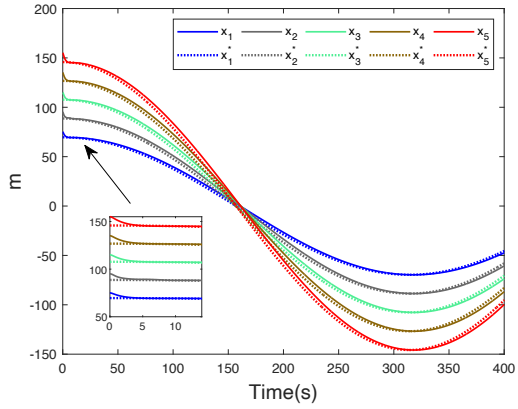

Fig. 4: Revolution of x-positions x_i and Nash equilibrium solutions x_i^*

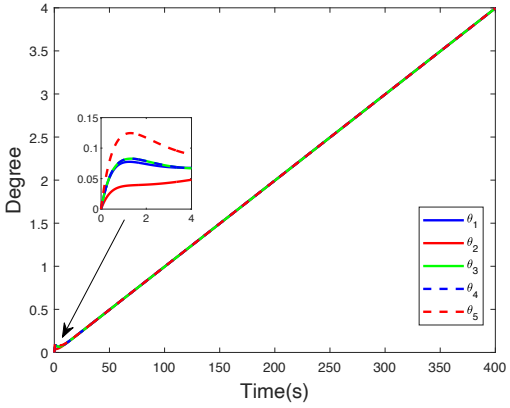

Fig. 7: Revolution of 5 ISVs player parameters θ_i

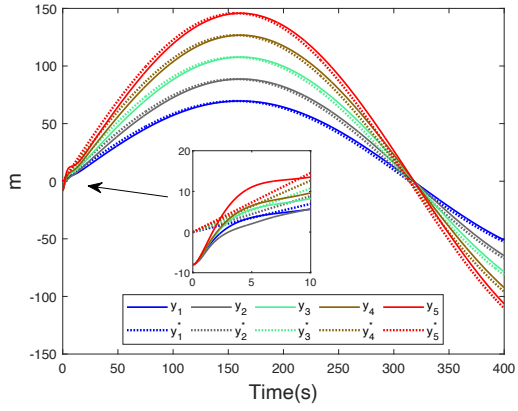

Fig. 5: Revolution of y-positions y_i and Nash equilibrium solutions y_i^*

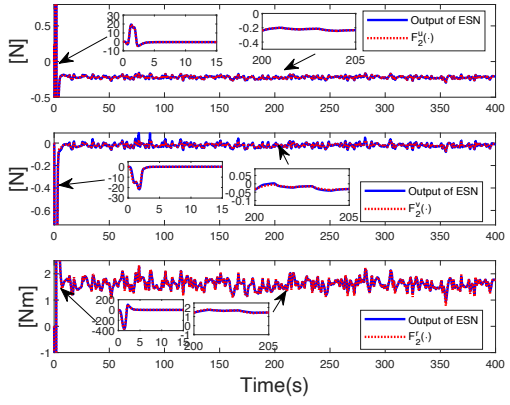

Fig. 8: Learning profile of echo state network (ESN) based on the proposed method

VI. Conclusion

In this paper, a distributed control method was presented based on the Nash equilibrium seeking approach for a swarm of ISVs to address the noncooperative game-based cooperative maneuvering problem. Action estimators were constructed based on a distributed observer design to estimate the actions of other ISVs. Accelerated learning-based neural predictors were constructed to identify the uncertainties in the model of vehicles, and adaptation laws for the output weights of echo state networks were designed by using a high-order tuner to accelerate the convergence rate. Kinematic control laws, kinetic control laws, and update laws of individual variables were developed by using the Nash equilibrium seeking

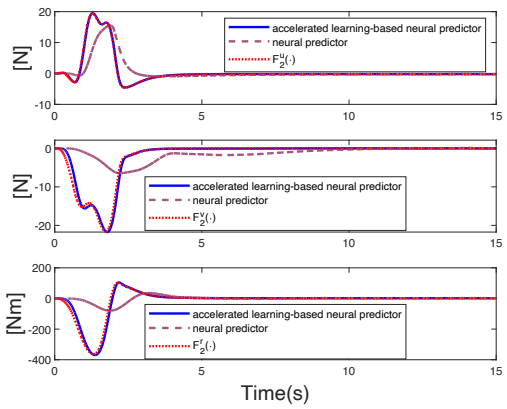

Fig. 9: Comparison between accelerated learning-based neural predictor and neural predictor

strategy. Based on the cascade system theory and input-to-state stability analysis, three subsystems and the resulting closed-loop system were proved to be input-to-state stable, and besides *Geometric Task* and *Dynamic Task* of cooperative maneuvering were achieved.

REFERENCES

[1] X. Wang, "Active fault tolerant control for unmanned underwater vehicle with actuator fault and guaranteed transient performance," *IEEE Transactions on Intelligent Vehicles*, vol. 6, no. 3, pp. 470–479, 2021.

[2] Y. Huang, S. Z. Yong, and Y. Chen, "Stability control of autonomous ground vehicles using control-dependent barrier functions," *IEEE Transactions on Intelligent Vehicles*, vol. 6, no. 4, pp. 699–710, 2021.

[3] S. Xiao, X. Ge, Q.-L. Han, and Y. Zhang, "Resource-efficient platooning control of connected automated vehicles over vanets," *IEEE Transactions on Intelligent Vehicles*, pp. 1–1, 2022.

[4] Y. Shi, C. Shen, H. Fang, and H. Li, "Advanced control in marine mechatronic systems: A survey," *IEEE/ASME Transactions on Mechatronics*, vol. 22, no. 3, pp. 1121–1131, 2017.

[5] X. Xiang, C. Yu, L. Lapierre, J. Zhang, and Q. Zhang, "Survey on fuzzy-logic-based guidance and control of marine surface vehicles and underwater vehicles," *International Journal of Fuzzy Systems*, vol. 20, no. 2, pp. 572–586, 2018.

[6] Z. Peng, J. Wang, D. Wang, and Q. Han, "An overview of recent advances in coordinated control of multiple autonomous surface vehicles," *IEEE Transactions on Industrial Informatics*, vol. 17, no. 2, pp. 732–745, 2021.

[7] N. Gu, D. Wang, Z. Peng, J. Wang, and Q.-L. Han, "Advances in line-of-sight guidance for path following of autonomous marine vehicles: An overview," *IEEE Transactions on Systems, Man, and Cybernetics: Systems*, 2022, doi: 10.1109/TSMC.2022.3162862.

[8] Y. Lu, G. Zhang, L. Qiao, and W. Zhang, "Adaptive output-feedback formation control for underactuated surface vessels," *International Journal of Control*, vol. 93, no. 3, pp. 400–409, 2020.

[9] S.-L. Dai, S. He, H. Cai, and C. Yang, "Adaptive leaderfollower formation control of underactuated surface vehicles with guaranteed performance," *IEEE Transactions on Systems, Man, and Cybernetics: Systems*, vol. 52, no. 3, pp. 1997–2008, 2022.

[10] S.-L. Dai, S. He, Y. Ma, and C. Yuan, "Cooperative learning-based formation control of autonomous marine surface vessels with prescribed performance," *IEEE Transactions on Systems, Man, and Cybernetics: Systems*, vol. 52, no. 4, pp. 2565–2577, 2022.

[11] W. Wu, Z. Peng, L. Liu, and D. Wang, "A general safety-certified cooperative control architecture for interconnected intelligent surface vehicles with applications to vessel train," *IEEE Transactions on Intelligent Vehicles*, 2022, accepted.

[12] L. Ma, Y.-L. Wang, and Q.-L. Han, "Cooperative target tracking of multiple autonomous surface vehicles under switching interaction topologies," *IEEE/CAA Journal of Automatica Sinica*, 2022, doi: 10.1109/JAS.2022.105509.

[13] B.-B. Hu and H.-T. Zhang, "Bearing-only motional target-surrounding control for multiple unmanned surface vessels," *IEEE Transactions on Industrial Electronics*, vol. 69, no. 4, pp. 3988–3997, 2022.

[14] Y. Jiang, Z. Peng, D. Wang, Y. Yin, and Q.-L. Han, "Cooperative target enclosing of ring-networked underactuated autonomous surface vehicles based on data-driven fuzzy predictors and extended state observers," *IEEE Transactions on Fuzzy Systems*, vol. 30, no. 7, pp. 2515–2528, 2022.

[15] Y. Zhang, D. Wang, and Z. Peng, "Consensus maneuvering for a class of nonlinear multivehicle systems in strict-feedback form," *IEEE Transactions on Cybernetics*, vol. 49, no. 5, pp. 1759–1767, 2018.

[16] Y. Zhang, D. Wang, Z. Peng, and T. Li, "Distributed containment maneuvering of uncertain multiagent systems in MIMO strict-feedback form," *IEEE Transactions on Systems, Man, and Cybernetics: Systems*, vol. 51, no. 2, pp. 1354–1364, 2021.

[17] Z. Peng, J. Wang, and D. Wang, "Containment maneuvering of marine surface vehicles with multiple parameterized paths via spatial-temporal decoupling," *IEEE/ASME Transactions on Mechatronics*, vol. 22, no. 2, pp. 1026–1036, Apr. 2017.

[18] Z. Peng, J. Wang, and D. Wang, "Distributed containment maneuvering of multiple marine vessels via neurodynamics-based output feedback," *IEEE Transactions on Industrial Electronics*, vol. 64, no. 5, pp. 3831–3839, May 2017.

[19] L. Liu, D. Wang, Z. Peng, and T. Li, "Modular adaptive control for LOS-based cooperative path maneuvering of multiple underactuated autonomous surface vehicles," *IEEE Transactions on Systems, Man, and Cybernetics: Systems*, vol. 47, no. 7, pp. 1613–1624, Jul. 2017.

[20] Z. Peng, J. Wang, and D. Wang, "Distributed maneuvering of autonomous surface vehicles based on neurodynamic optimization and fuzzy approximation," *IEEE Transactions on Control Systems Technology*, vol. 26, no. 3, pp. 1083–1090, 2018.

[21] M. Fu and L. Wang, "Finite-time coordinated path following control of underactuated surface vehicles based on event-triggered mechanism," *Ocean Engineering*, vol. 246, p. 110530, 2022.

[22] Y. Zhang, D. Wang, Y. Yin, and Z. Peng, "Event-triggered distributed coordinated control of networked autonomous surface vehicles subject to fully unknown kinetics via concurrent-learning-based neural predictor," *Ocean Engineering*, vol. 234, p. 108966, 2021.

[23] L. Liu, D. Wang, Z. Peng, and Q.-L. Han, "Distributed path following of multiple under-actuated autonomous surface vehicles based on data-driven neural predictors via integral concurrent learning," *IEEE Transactions on Neural Networks and Learning Systems*, vol. 32, no. 12, pp. 5334–5344, 2021.

[24] Y. Zhao, Y. Ma, and S. Hu, "USV formation and path-following control via deep reinforcement learning with random braking," *IEEE Transactions on Neural Networks and Learning Systems*, vol. 32, no. 12, pp. 5468–5478, 2021.

[25] X. Gong, L. Liu, Z. Peng, D. Wang, and W. Zhang, "Resource-aware synchronized path following of multiple unmanned surface vehicles with experiments: A cooperative vector field approach," *Control Engineering Practice*, vol. 124, p. 105184, 2022.

[26] G. Zhang, C. Huang, J. Li, and X. Zhang, "Constrained coordinated path-following control for underactuated surface vessels with the disturbance rejection mechanism," *Ocean Engineering*, vol. 196, p. 106725, 2020.

[27] Z. Peng, D. Wang, T. Li, and M. Han, "Output-feedback cooperative formation maneuvering of autonomous surface vehicles with connectivity preservation and collision avoidance," *IEEE Transactions on Cybernetics*, vol. 50, no. 6, pp. 2527–2535, 2020.

[28] N. Gu, D. Wang, Z. Peng, and J. Wang, "Safety-critical containment maneuvering of underactuated autonomous surface vehicles based on neurodynamic optimization with control barrier functions," *IEEE Transactions on Neural Networks and Learning Systems*, pp. 1–14, 2021.

[29] M. Ye and G. Hu, "Distributed Nash equilibrium seeking by a consensus based approach," *IEEE Transactions on Automatic Control*, vol. 62, no. 9, pp. 4811–4818, 2017.

[30] ——, "Distributed nash equilibrium seeking in multiagent games under switching communication topologies," *IEEE Transactions on Cybernetics*, vol. 48, no. 11, pp. 3208–3217, 2018.

[31] Z. Deng, "Distributed nash equilibrium seeking for aggregative games with second-order nonlinear players," *Automatica*, vol. 135, p. 109980, 2022.

[32] X. Ai and L. Wang, "Distributed adaptive nash equilibrium seeking and disturbance rejection for noncooperative games of high-order nonlinear systems with input saturation and input delay," *International Journal of Robust and Nonlinear Control*, vol. 31, no. 7, pp. 2827–2846, 2021.

[33] G. Wen, X. Fang, J. Zhou, and J. Zhou, "Robust formation tracking of multiple autonomous surface vessels with individual objectives: A

noncooperative game-based approach," *Control Engineering Practice*, vol. 119, p. 104975, 2022.
[34] X. Fang, J. Zhou, and G. Wen, "Location game of multiple unmanned surface vessels with quantized communications," *IEEE Transactions on Circuits and Systems II: Express Briefs*, vol. 69, no. 3, pp. 1322–1326, 2022.
[35] V. Nikiforov, D. Gerasimov, and A. Pashenko, "Modular adaptive backstepping design with a high-order tuner," *IEEE Transactions on Automatic Control*, vol. 67, no. 5, pp. 2663–2668, 2022.
[36] S. SMcDonald, Y. Cui, J. E. Gaudio, and A. M. Annaswamy, "A high-order tuner for accelerated learning and control," *arXiv preprint arXiv:2103.12868*, 2021.
[37] J. E. Gaudio, A. M. Annaswamy, J. M. Moreu, M. A. Bolender, and T. E. Gibson, "Accelerated learning with robustness to adversarial regressors," in *Learning for Dynamics and Control*. PMLR, 2021, pp. 636–650.
[38] J. Nash, "Non-cooperative games," *Annals of Mathematics*, vol. 54, no. 2, pp. 286–295, 1951.
[39] A. R. Romano and L. Pavel, "Dynamic ne seeking for multi-integrator networked agents with disturbance rejection," *IEEE Transactions on Control of Network Systems*, vol. 7, no. 1, pp. 129–139, 2020.
[40] Y. Zhang, S. Liang, X. Wang, and H. Ji, "Distributed Nash equilibrium seeking for aggregative games with nonlinear dynamics under external disturbances," *IEEE Transactions on Cybernetics*, vol. 50, no. 12, pp. 4876–4885, 2020.
[41] Q. Wei, L. Zhu, R. Song, P. Zhang, D. Liu, and J. Xiao, "Model-free adaptive optimal control for unknown nonlinear multiplayer nonzero-sum game," *IEEE Transactions on Neural Networks and Learning Systems*, vol. 33, no. 2, pp. 879–892, 2022.
[42] H. Jaeger, "The echo state approach to analysing and training recurrent neural networks-with an erratum note," *Bonn, Germany: German National Research Center for Information Technology GMD Technical Report*, vol. 148, no. 34, p. 13, 2001.
[43] Z. Peng, D. Wang, T. Li, and Z. Wu, "Leaderless and leader-follower cooperative control of multiple marine surface vehicles with unknown dynamics," *Nonlinear Dynamics*, vol. 74, no. 1-2, pp. 95–106, 2013.
[44] A. Levant, "Robust exact differentiation via sliding mode technique," *Automatica*, vol. 34, no. 3, pp. 379–384, 1998.
[45] M. Krstic, I. Kanellakopoulos, and P. V. Kokotovic, *Nonlinear and Adaptive Control Design*. John Wiley & Sons, 1995.
[46] H. K. Khalil, *Nonlinear Control*. Pearson Education, 2015.
[47] T. I. Fossen, *Handbook of marine craft hydrodynamics and motion control*. John Wiley & Sons, 2011.

Yibo Zhang (Member, IEEE) received the B.E. degree in marine electronic and electrical engineering and the Ph. D. degree in marine electrical engineering from Dalian Maritime University, Dalian, China, in 2014 and 2021. He is a Postdoctoral Fellow with the Department of Automation, Shanghai Jiao Tong University.

His current research interests include cooperative control and intelligent control of multi-agent systems and multiple marine vehicles.

Wentao Wu (Student Member, IEEE) received the B.E. degree in electrical engineering and automation from Harbin University of Science and Technology, Harbin, China, in 2018. He received the M.E. degree in electrical engineering from Dalian Maritime University, Dalian, China, in 2021. He is pursing the Ph.D. degree in electronic information from Shanghai Jiao Tong University, Shanghai, China.

His current research interests include unmanned surface vehicles, formation control, adaptive control, and safety control.

Weidong Zhang (Senior Member, IEEE) received his BS, MS, and PhD degrees from Zhejiang University, China, in 1990, 1993, and 1996, respectively, and then worked as a Postdoctoral Fellow at Shanghai Jiaotong University.

He joined Shanghai Jiaotong University in 1998 as an Associate Professor and has been a Full Professor since 1999. From 2003 to 2004 he worked at the University of Stuttgart, Germany, as an Alexander von Humboldt Fellow. He is a recipient of National Science Fund for Distinguished Young Scholars, China and Cheung Kong Scholar, Ministry of Education, China. He is currently Director of the Engineering Research Center of Marine Automation,Shanghai Municipal Education Commission, and Director of Marine Intelligent System Engineering Research Center, Ministry of Education, China. His research interests include control theory, machine learning theory, and their applications in industry and autonomous systems. He is the author of 265 SCI papers and 1 book, and holds 72 patents.